

# Magnetoresistance of LaCoO<sub>3</sub> and an Insulator–Metal Transition Induced in It by a High Magnetic Field

S. G. Ovchinnikov<sup>a–c</sup> and Yu. S. Orlov<sup>a,\*</sup>

<sup>a</sup> Kirensky Institute of Physics, Siberian Branch, Russian Academy of Sciences,  
Akademgorodok, Krasnoyarsk, 660036 Russia

\* e-mail: js0.krasn@mail.ru

<sup>b</sup> Siberian Federal University, Svobodnyi pr. 79, Krasnoyarsk, 660041 Russia

<sup>c</sup> Reshetnev Siberian State Aerospace University, Krasnoyarsk, 660014 Russia

Received September 24, 2010

The transformation of the band structure of LaCoO<sub>3</sub> in the applied magnetic field has been theoretically studied. If the field is below its critical value  $B_C \approx 65$  T, the dielectric band gap decreases with the field, thus giving rise to negative magnetoresistance that is highest at  $T = 300–500$  K. The critical field is related to the crossover between the low- and high-spin terms of Co<sup>3+</sup> ions. The spin crossover results in an insulator–metal transition induced by an increase in the magnetic field.

DOI: 10.1134/S0021364010210095

With the growth of the temperature, the LaCoO<sub>3</sub> compound behaves as a nonmagnetic insulator, then as a paramagnetic insulator, and finally as a paramagnetic metal [1, 2]. The transitions between these states are gradual and smeared; they are crossovers rather than conventional phase transitions. A mechanism underlying the insulator–metal transition observed in LaCoO<sub>3</sub> within the 500–600 K temperature range was recently proposed in [3], where the electron structure of LaCoO<sub>3</sub> at finite temperatures was calculated using the LDA + GTB method [4], which is an implementation of Hubbard's ideas in the case of many-electron and multiorbital systems. The description of an electron in a strongly correlated system in terms of a linear combination of Hubbard fermions (quasiparticle excitations between different many-electron states; see Fig. 1) made it possible to calculate and analyze the characteristic features of the band structure. The energy spectrum of LaCoO<sub>3</sub> exhibit midgap states related to the transitions from the excited high-spin state for the d<sup>6</sup> configuration to the ground high-spin state for the d<sup>5</sup> configuration (see dashed lines in Fig. 1). These states effectively reduce the dielectric band gap  $E_g$  with the growth of temperature. The spectral weight of the quasiparticle excitations is determined by the occupation of many-electron states. The first excited level of the high-spin term for the d<sup>6</sup> configuration is separated by a small spin gap  $\Delta_{s-t} \approx 150$  K from the low-spin <sup>1</sup>A<sub>1</sub> term [5–7] (Fig. 1). Therefore, the thermally-induced occupation of the excited states increasing with  $T$  leads to the growth of both the magnetic susceptibility and the band width characterizing the midgap states. In the present paper, we demon-

strate that the applied magnetic field reduces the spin gap thus inducing the transition of LaCoO<sub>3</sub> to the metallic state.

The applied magnetic field splits the triply degenerate  $\tilde{J} = 1$  level and the fivefold degenerate  $\tilde{J} = 2$  level of the <sup>5</sup>T<sub>2</sub> term corresponding to the d<sup>6</sup> configuration, as is shown in Fig. 2. At a critical value of the magnetic field ( $B_C \approx 65$  T) [5], there occurs a crossover between the ground-state low-spin orbital <sup>1</sup>A<sub>1</sub> singlet and the sublevel characterized by the effective angular momentum  $\tilde{J} = 1$  and the projection  $m_{\tilde{J}=1} = 1$

$$\Delta_{s-t}(B) = \Delta_{s-t}(0) - g\mu B,$$

where  $\mu$  is the Bohr magneton and  $g = 3.4$  is the g factor [5–7]. Level crossing induces the magnetic transition reported in [8], which was observed in LaCoO<sub>3</sub> in the course of magnetization measurements. The critical field corresponds to the transition point. The splitting of levels in the applied magnetic field leads to the redistribution of their thermally-induced occupation and hence to the redistribution of the spectral weights of the quasiparticle excitations related to the transitions from the states with different projections of the angular momentum:  $m_{\tilde{J}=1} = 0, \pm 1$ , and  $m_{\tilde{J}=2} = 0, \pm 1, \pm 2$ . The applied magnetic field lifts the degeneracy of the many-electron states. Therefore, in the GTB scheme, we take into account the level splitting in all  $d^{n-1}$ ,  $d^n$ , and  $d^{n+1}$  configurations under study. In contrast to the applied or chemical pressure, the magnetic field reduces the characteristic energy of the singlet–triplet transition and leads to a temperature-induced

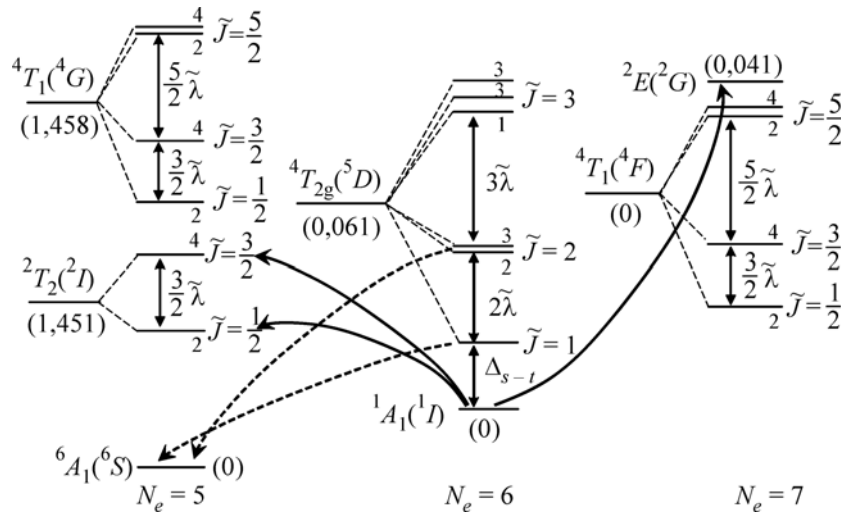


**Fig. 1.** Set of low-energy terms for  $d^{N_e}$  ( $N_e = 5, 6$ , and  $7$ ) electronic configurations in the crystal field. At  $T = 0$  K, only the ground-state low-spin  $^1A_1$  ( $N_e = 6$ ) singlet is occupied. The fermionic excitations forming the bottom of the conduction band and the top of the valence band are shown by solid lines. Dashed lines denote the transitions responsible for the formation of the mid-gap states with the growth of temperature. Their spectral weight is determined by the occupation of the excited high-spin state corresponding to the  $d^6$  configuration. The energy values (in electron volts) with respect to the lowest level of each configuration are given in brackets. For each of three subspaces of the Hilbert space, we choose its own energy reference point.

increase in the activation rate for the midgap states in the band spectrum.

At very low temperatures, the insulator–metal transition induced by the magnetic field is of special interest. At  $T = 0$  K and the applied magnetic field below its critical value,  $B < B_C$ , the only term being occupied is the ground-state low-spin singlet  $^1A_1$ . The band structure formed by  $d^6 \ ^1A_1 \longrightarrow d^5 \ ^2T_2 \ \tilde{J} = 1/2$ ,  $\tilde{J} = 3/2$  transitions (for the valence band) and  $d^6$

$^1A_1 \rightarrow d^7/2 E$  (for the conduction band) (see solid lines in Fig. 1), exhibits a dielectric band gap (Fig. 3a) [3]. However, at  $B > B_C$ , the low-spin  $|d^6\ ^5T_2 \tilde{J} = 1, m_{\tilde{J}=1} = 1\rangle$  state turns out to be the ground state (Fig. 2). The quasiparticle transitions  $d^6\ ^5T_2 \tilde{J} = 1, m_{\tilde{J}=1} = 1 \rightarrow d^7/4 T_1 \tilde{J} = 1/2, \tilde{J} = 3/2, \tilde{J} = 5/2$  and the similar  $d^5(^4T_1)$  term give rise to the valence and conduction bands. The  $d^6\ ^5T_2 \tilde{J} = 1, m_{\tilde{J}=1} = 1 \rightarrow d^5\ ^6A_1$  transitions forming the midgap states have the largest spectral weight and the band structure is of a metallic type (Fig. 3b). The band gap vanishes at the  $\Gamma$  point. Note that the field-induced transition at  $T = 0$  is a Lifshitz phase transition [9]. The density of states at the Fermi level and the Sommerfeld parameter  $\gamma = C_e/T$  (where  $C_e$  is the electronic specific heat) have a singularity of the  $(B - B_C)^{1/2}$  type. This transition is characterized by the topological order parameter [10].

At finite temperatures within the range  $kT \sim |B - B_C|$ , both low-spin  $^1A_1$  and high-spin  $^5T_2$  terms belonging to the  $d^6$  configuration are occupied. As a result, the contribution of the midgap states to the band structure manifests itself, even at  $B < B_C$ , and the transition is smeared. Therefore, at a finite temperature, we observe a smooth crossover instead of a phase transition.

In Fig 4a, we present the temperature dependence of the dielectric band gap  $E_g$  at different values of the applied magnetic field  $B$ . It is clear that the growth of

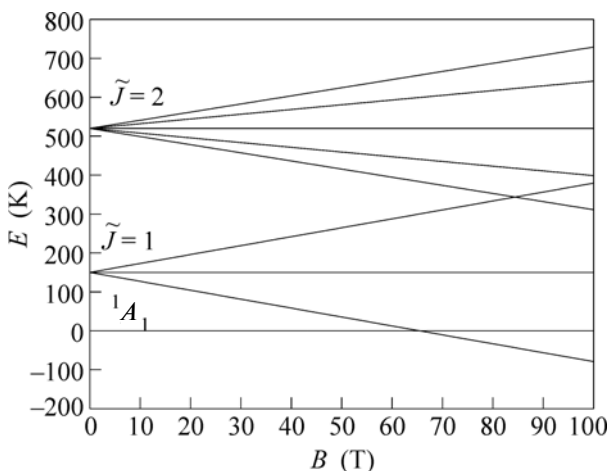


**Fig. 2.** Energies of the low-lying states of the  $\text{Co}^{3+}$  ion in the applied magnetic field.

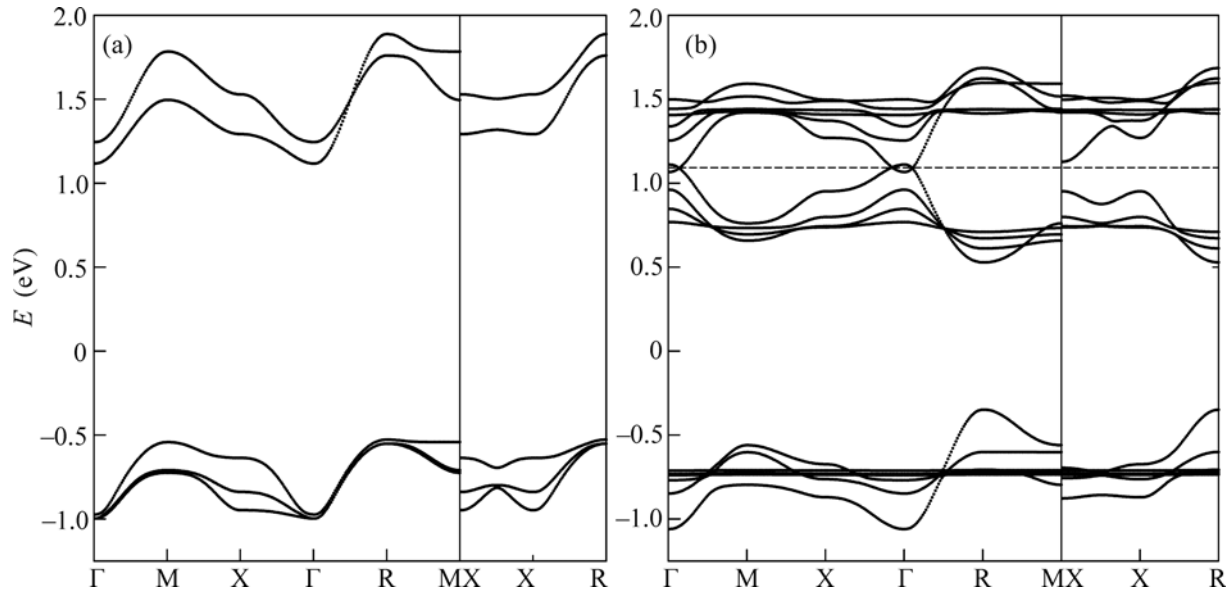


**Fig. 3.** Quasiparticle spectrum at  $T = 0$  K and at magnetic field (a)  $B < B_C$  and (b)  $B > B_C$ . The dashed line shows the chemical potential.

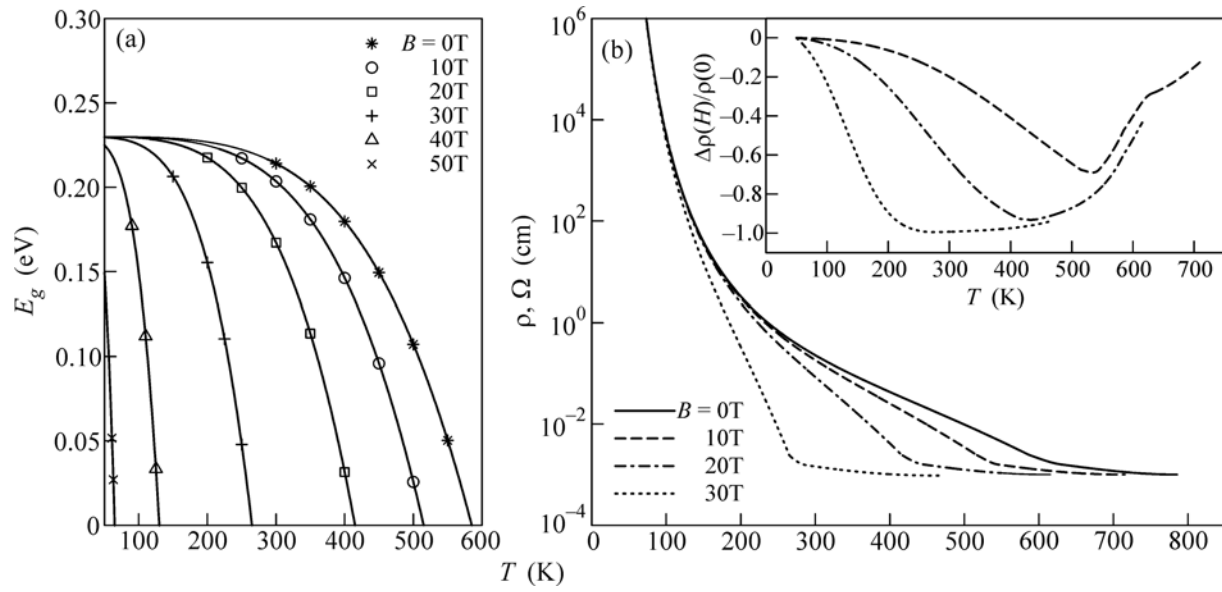


**Fig. 4.** Temperature dependences of the (a) dielectric band gap and (b) electrical resistance for various magnetic fields. The temperature dependence of the magnetoresistance  $\Delta\rho/\rho = (\rho(B) - \rho(0))/\rho(0)$  at the same values of the applied magnetic field is shown in the inset.

the temperature and magnetic field favors the decrease in  $E_g$ . The characteristic temperature  $T_{IMT}$  (the temperature, at which  $E_g$  vanishes) of the transition from the insulating to metallic state decreases in the applied magnetic field.

Following the line of reasoning presented in paper [3], we obtained the temperature dependence of the

electrical resistance at various values of the magnetic field within the range of existence for the insulating state  $B < B_C$  (Fig. 4b). In the inset of Fig. 4b, we show the temperature dependence of magnetoresistance  $(\rho(B) - \rho(0))/\rho(0)$ . Here, the magnetoresistance is negative and attains its maximum absolute value of about 100% in the 300–500 K temperature range at

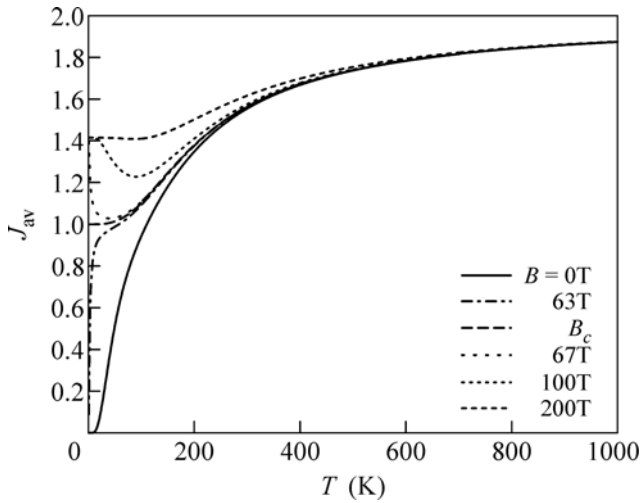


**Fig. 5.** Temperature dependence of the average angular momentum at different values of the applied magnetic field  $B$ . With the growth of temperature, a transition from the nonmagnetic low-spin state characteristic of  $T \approx 0$  K to the paramagnetic state occurs. At the spin transition temperature  $T \sim 100$  K, we have  $J_{\text{av}} \approx 1$ .

moderate magnetic fields. At the applied magnetic field  $B$  as high as 30 T, the minimum of the magnetoresistance is located near room temperature.

The average value of the angular momentum squared can be written in the form [3]

$$\begin{aligned} \langle \hat{J}^2 \rangle &= \sum_{pq} \langle p | \hat{J}^2 | q \rangle \langle X^{pq} \rangle \\ &= \sum_N \sum_{p(N)} \langle p(N) | \hat{J}^2 | p(N) \rangle \langle X^{p(N)p(N)} \rangle, \end{aligned}$$

where the sum over  $N$  is the sum over the sectors of the Hilbert space ( $N = 5, 6$ , and  $7$ );  $|p\rangle$  and  $|q\rangle$  are the eigenstates of the  $\hat{J}^2$  operator (Fig. 1), i.e.,  $\hat{J}^2 |p\rangle = J(J+1) |p\rangle$ ; and  $X^{pq}$  are the Hubbard  $X$ -operators constructed on the basis of  $|p\rangle$  and  $|q\rangle$  states.

As a measure for the average value of the angular momentum operator, let us take the square root of the average value of the angular momentum squared

$$J_{\text{av}} = \sqrt{\langle \hat{J}^2 \rangle}.$$

Since the averages  $\langle X^{pp} \rangle$  depend on temperature and magnetic field,  $J_{\text{av}}$  is also a function of temperature and magnetic field (Fig. 5).

At low temperatures and zero magnetic field (solid line in Fig. 5), the average value of the angular momentum is nearly zero. This corresponds to the nonmagnetic state of  $\text{LaCoO}_3$ . The value  $J_{\text{av}} \approx 2$  expected for the high-spin state is achieved only at  $T \approx$

1000 K. At a temperature of 100 K, the average value of the angular momentum is close to unity. In our opinion, this can be a source of the widespread erroneous viewpoint, according to which the intermediate-spin state makes the dominant contribution to the spin transition occurring in  $\text{LaCoO}_3$  at 100 K [11–13].

Let us now consider the behavior of  $J_{\text{av}}$  with an increase in the applied magnetic field. It seems better to begin with the case of  $T = 0$ . The averages  $\langle X^{p(N)p(N)} \rangle$  are proportional to the thermally induced occupation of the  $|p(N)\rangle$  states. At zero doping, a nonvanishing contribution comes from the averages with  $N = 6$ ; hence,  $J_{\text{av}} = 0$  at  $B < B_C$ . At the crossover point  $B = B_C$ , the nonmagnetic  ${}^1A_1$  state and magnetic high-spin state with  $J_{\text{av}} = 1$  are occupied with the equal probabilities of  $1/2$ , whereas at  $B > B_C$ ,  $J_{\text{av}} = \sqrt{2}$ , since the high-spin  $|\tilde{J} = 1, m_{\tilde{J}} = 1\rangle$  state becomes the ground state. With the growth of temperature at  $B < B_C$ ,  $J_{\text{av}}$  first tends to unity up to  $T \approx 100$  K (as well as in zero field) and then to  $J_{\text{av}} = 2$  at  $T \approx 1000$  K. At  $B > B_C$ , the first thermally excited state is the nonmagnetic  ${}^1A_1$  state; therefore, the temperature dependence of  $J_{\text{av}}$  first exhibits a dip, which becomes smaller at higher magnetic fields, and then  $J_{\text{av}}$  increases with the temperature.

In conclusion, note that the magnetic field dependence of many-electron terms of the  $\text{Co}^{3+}$  ion leads to the spin crossover at  $B = B_C \approx 65$  T. At  $B < B_C$ , the field-induced narrowing of the spin gap leads to a large (of about 100%) negative magnetoresistance. At  $B > B_C$ ,  $\text{LaCoO}_3$  is in the metallic state. All these theoretical predictions could be tested in experiments since the critical magnetic field equal to 65 T is currently accessible.

This work was supported by the Division of Physical Sciences, Russian Academy of Sciences (program no. 2.3); by the Siberian and Ural Branches, Russian Academy of Sciences (joint project no. 40); by the Ministry of Education and Science of the Russian Federation (state contract no. P891, federal program “Scientific and Pedagogical Personnel of Innovative Russia”); by the Russian Foundation for Basic Research (project nos. 09-02-00171 and 10-02-00251); and by the Dynasty Foundation.

## REFERENCES

1. M. Tachibana, T. Yoshida, H. Kawaji, et al., Phys. Rev. B **77**, 094402 (2008).
2. J. Baier, S. Jodlauk, M. Kriener, et al., Phys. Rev. B **71**, 014443 (2005).

3. S. G. Ovchinnikov, Yu. S. Orlov, I. A. Nekrasov, and Z. V. Pchelkina, *Zh. Eksp. Teor. Fiz.* **138** (6) (2010, in press).
4. M. M. Korshunov, V. A. Gavrichkov, S. G. Ovchinnikov, et al., *Phys. Rev. B* **72**, 165104 (2005).
5. S. Noguchi, S. Kawamata, K. Okuda, et al., *Phys. Rev. B* **66**, 094404 (2002).
6. M. J. R. Hoch, S. Nellutla, J. van Tol, et al., *Phys. Rev. B* **79**, 214421 (2009).
7. Z. Ropka and R. J. Radwanski, *Phys. Rev. B* **67**, 172401 (2003).
8. K. Sato, A. Matsuo, K. Kindo, et al., *J. Phys. Soc. Jpn.* **78**, 093702 (2009).
9. I. M. Lifshitz, *Zh. Eksp. Teor. Fiz.* **38**, 1569 (1960) [Sov. Phys. JETP] **11**, 1130 (1960)].
10. G. Volovik, *Lect. Notes Phys.* **718**, 31 (2007).
11. M. A. Korotin, S. Yu. Ezhov, I. V. Solovyev, et al., *Phys. Rev. B* **54**, 5309 (1996).
12. K. Asai, A. Yoneda, O. Yokokura, et al., *J. Phys. Soc. Jpn.* **67**, 290 (1998).
13. T. Saitoh, T. Mizokawa, A. Fujimori, et al., *Phys. Rev. B* **55**, 4257 (1997).

*Translated by K. Kugel*